Geochimica et Cosmochimica Acta Vol. 44, pp. 685 to 699

0016-7037/80/0501-0685$02.00/0

Mineralogy and petrography of HAL, an isotopically-unusual Allende inclusion

JOHN M. ALLEN*
Department of the Geophysical Sciences, University of Chicago, Chicago, IL 60637, U.S.A.

LAWRENCE GROSSMAN
Department of the Geophysical Sciences and Enrico Fermi Institute, University of Chicago, IL 60637, U.S.A.

TYPHOON LEE†
Enrico Fermi Institute, University of Chicago, IL 60637, U.S.A.

and

G. J. WASSERBURG
Lunatic Asylum, Division of Geological and Planetary Sciences, California Institute of Technology, Pasadena, CA 91109, U.S.A.

(*Received* 17 *July* 1979; *accepted in revised form* 9 *January* 1980)

Abstract—A detailed mineralogical study of HAL was initiated to elucidate the origin of this inclusion because LEE *et al.* (1979) had found large mass fractionation effects and small nuclear effects in its Ca isotopic composition, but no ^{26}Mg excesses in samples of it with very high $^{27}Al/^{24}Mg$ ratios. HAL's 1.0 mm radius interior consists almost entirely of three hibonite crystals and is surrounded by a 2.0 mm thick, multi-layered rim. The first layer, called the black rim, is black and compact, resembles a devitrified glass and contains an anisotropic Al–Fe-oxide similar to hercynite in composition. This is followed by a friable rim sequence, layer I of which is predominantly feldspathoids with minor anorthite, Ti–Fe-oxide and Al–Fe-oxide. Layer II contains abundant perovskite, plus grossular, andradite and pyroxene in addition to the minerals of layer I. Layer III is mostly Ca-phosphate, possibly hydroxy-apatite, and perovskite. Layer IV is rich in hibonite, Al–Fe-oxide, perovskite, nepheline and the two garnets, lacks Ca-phosphate but contains traces of a Ti–Sc–Zr-oxide. Layer V is rich in Al–Fe-oxide, pyroxene, nepheline, the two garnets and olivine whose crystals display peculiar rectangular cross-sections. The black rim does not completely surround the hibonite core. Sectors of the friable rim exist where layer I is missing and where the mineralogy of adjacent layers is no different from that of the same layers in other sectors. Pentlandite, nickel-iron and barrel-shaped olivine crystals, minerals typical of the matrix of Allende and found nowhere else in HAL, are found in layer V and increase in abundance toward its exterior, as if grains of these phases accreted together with the other minerals of layer V. This layer also contains alternating olivine-rich and garnet-, pyroxene-rich bands, resembling rhythmic layering. For these reasons, we conclude that each of the layers of the friable rim formed by the accretion of an assemblage of condensate grains rather than by complete reaction of a precursor to HAL with a nebular gas. Thus, the unusual isotopic characteristics of HAL are thought to have been inherited from a nebular reservoir which was isotopically distinct from that which gave rise to the bulk of the material in Allende. HAL's mineralogical peculiarities indicate that its formation reservoir was also chemically distinct from the latter one.

INTRODUCTION

THERE IS a substantial body of evidence that Ca–Al-rich inclusions in C2 and C3 chondritic meteorites contain high-temperature material that formed very early during condensation of the solar nebula (LARIMER and ANDERS, 1970; MARVIN *et al.*, 1970; GROSSMAN, 1972; 1973). Condensation calculations predict various aluminum oxides to be the highest temperature condensates of the major elements (GROSSMAN, 1972; BLANDER and FUCHS, 1975). Of the aluminum oxide species predicted, only hibonite ($CaAl_{12}O_{19}$) has been found in Ca–Al-rich inclusions. The others, corundum and $CaAl_4O_7$, have not been found and may be unstable in cosmic gases. Hibonite, on the basis of its estimated free energy of formation (BLANDER and FUCHS, 1975) and its textural relations in Ca–Al-rich inclusions (ALLEN *et al.*, 1978) may be the highest temperature, major element condensate. Studies of hibonite-rich Allende inclusions may thus reveal important information about chemical processes which took place at the initiation of condensation and which may not be recorded in hibonite-free inclusions.

* Present address: Dept. of Geology, University of Toronto, Toronto, Ontario, Canada M5S 1A1.
† Present address: Dept. of Terrestrial Magnetism, Carnegie Institution of Washington, 5241 Broad Branch Rd., NW, Washington, DC 20015, U.S.A.

HAL, a remarkable Allende inclusion whose mineralogy is dominated by hibonite, was found by LEE *et al.* (1979) to have isotopic characteristics which differ from those of other inclusions in this meteorite: no ^{26}Mg excesses were detected, in spite of enormous $^{27}Al/^{24}Mg$ ratios in some samples, but large mass fractionation effects, coupled with small nuclear effects, were discovered in its Ca. We report here the results of a detailed mineralogical and textural study of HAL which shows that the unusual history of this inclusion indicated by its isotopic composition is reflected in a number of exceptional mineralogical peculiarities. Preliminary results of a detailed chemical study of HAL are given in TANAKA *et al.* (1979). A more complete report is in preparation and will appear later.

TECHNIQUES

The inclusion was discovered by one of us (T.L.) in a large fragment of the Allende meteorite being prepared for analysis in the laboratory of Dr E. Anders who generously permitted its removal for study. Its appearance in the meteorite surface was distinctive, consisting of a tiny (1.9 mm dia), white interior which contained only three crystals and an unusually thick (up to 2 mm) multi-layered rim. The interior crystals proved to be hibonite and the inclusion was therefore named HAL (Hibonite ALlende) by LEE *et al.* (1979).

The inclusion was removed from the meteorite by G. J. W. at Caltech using stainless steel tools. Fragments selected for making polished thin sections were: one showing the complete sequence from interior hibonite through the rim layers to Allende matrix; another containing a complete 700 μm hibonite crystal with some attached rim material; and twelve smaller fragments, 100–1000 μm in size, representing all texturally distinct regions of the inclusion. Mineral analyses were obtained with the University of Chicago electron microprobe using wavelength dispersion (or energy dispersion, where specified). The fine grain size of the rim layers necessitated study by the Chicago SEM fitted with a Si (Li) X-ray detector. Further details of analytical procedure and operating conditions may be found in ALLEN *et al.* (1978).

TEXTURE AND MINERALOGY

General description

HAL is a sub-spherical inclusion with a maximum diameter of 5 mm. It consists of three mineralogically and texturally distinct portions (Figs 1, 2) which, from the inside of the inclusion to the outside, are: (1) a coarsely crystalline, white interior, with (2) a narrow, black, compact, vitreous-looking rim and (3) a thick, multi-layered, fine-grained and friable outer rim zone (stippled in Fig. 1). Some mechanical disruption of the friable rim, presumably during compaction of the Allende parent body, has taken place. This is illustrated in the upper left-hand corner of Fig. 1 where the rim is intercepted by a nearby chondrule and part of the rim disappears adjacent to it.

Interior

The interior portion of HAL has a maximum diameter of 1.9 mm and consists almost entirely of three large (up to 1 mm dia) crystals of hibonite (Fig. 1). The two largest ones are approximately hexagonal in form, are in mutual contact and are partially enveloped by a black rim. A third crystal is elongated and may be a hexagonal plate viewed edge-on. It and a smaller, adjacent, fourth crystal are free of any black rim and separated from the larger hibonites by friable rim material. The latter two are bounded by crystal faces on all sides. Each crystal is roughly hexagonal in outline and consists of a white, frosty core containing fine needles of a Ti-rich phase, surrounded by a colorless, transparent rim (Fig. 3). The needles are very abundant, but constitute $\ll 50\%$ by volume of the core. They are $\ll 1$ μm in dia, precluding precise chemical analysis, but their Ti-rich composition, very high relief and birefringence and parallel extinction suggest they are rutile. The needles have their long axes oriented in three directions at 120° to one another in the (0001) plane of the hibonite and must, therefore, be exsolution products from the hibonite.

In one hibonite grain examined by SEM (Fig. 4), a crystal face was seen to be dotted with numerous hexagonal pits, 2–6 μm in size, defined by negative crystal faces. The pits are apparently completely free of extraneous material, such as glass. Alkali-rich phases, possibly nepheline and/or sodalite, have been deposited as thin films on the hibonite crystal surfaces and partially overgrow some of the pits. This material sometimes shows crystal faces which, together with its discontinuous distribution and the apparent absence of associated glass, suggests deposition from a vapor phase.

Black rim

Adhering to the surface of two of the interior hibonite grains is a discontinuous rim, up to 300 μm thick, of a black, compact material with conchoidal fracture and vitreous luster (Figs 1, 2). This material is thickest in depressions in and between the grains, thinner or absent over outwardly-projecting corners of crystals and in places has a bulging exterior surface. These factors combine to suggest that it may have been a liquid, its preferential concentration in hollows resulting from a tendency to minimize the liquid surface free energy. Figure 1 shows that approximately one-quarter of the exposed hibonite surfaces are free of black rim material, even though they possess depressions into which liquid could have flowed. Thus, if melt were ever present in this region, it is unlikely that it disappeared from here by flowing around to the other side of the hibonite core.

Microprobe work shows that the bulk of the black rim material is composed of an Al–Fe-oxide. In thin section, the oxide is olive-brown with high relief, low to moderate birefringence, wavy extinction and a grain size of 20–80 μm. LEE *et al.* (1979) found that it dissolves easily in a mixture of concentrated HNO_3 and HF. The black rim is cross-cut by fracture-filling veins containing nepheline, sodalite and anorthite (Fig. 2). In addition, SEM views reveal complex mottled and feathery textures (Fig. 5) in which the different areas contain different amounts of Na, Si, Ca and Cl, presumably due to differing amounts of very fine-grained, admixed nepheline, sodalite and anorthite which could not be resolved at 4000×. The mottling and featheriness are strongly reminiscent of textures seen in devitrified glasses. We therefore conclude that the once-molten black rim cooled to a glass and later devitrified. Because the feldspathoids are late-crystallizing alteration products found throughout the inclusion, they may not be the original devitrification products.

The inner surface of the black rim is irregular, with numerous rounded protuberances of hibonite into black material and vice versa. This suggests that the black rim is a later replacement product of the hibonite. Such a disequilibrium relationship clearly indicates that the immediate liquid precursor of the black rim was not a primary liquid from which the hibonite could have crystallized. In those regions of the hibonite surfaces where black rim is absent, the hibonite has smooth, uncorroded crystal faces (Fig. 1). This suggests that melt was never present in those regions, precluding the possibility that black rim material was once

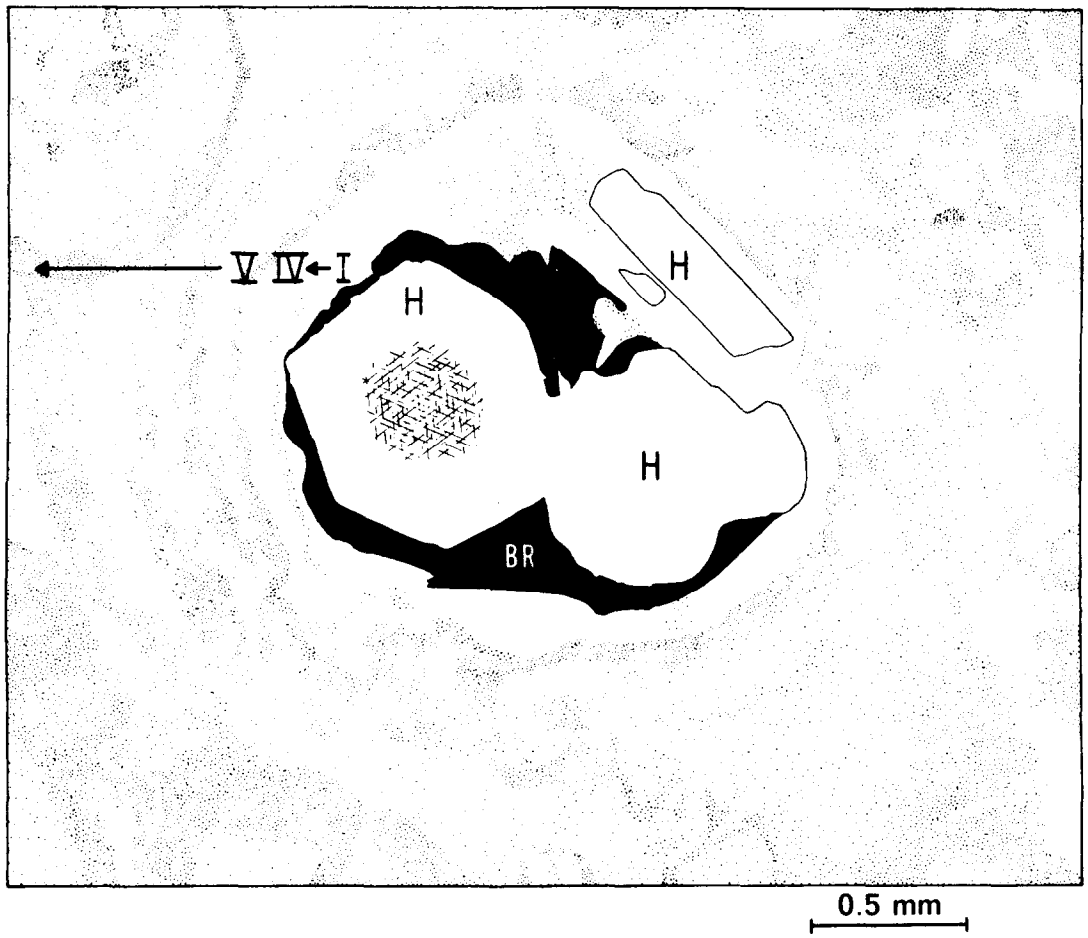

Fig. 1. The inclusion HAL in Allende. Hibonite crystals (H), one with exsolved needles of a Ti-rich phase oriented in three directions, are surrounded by a compact black rim (BR) and a friable, multi-layered rim sequence (I → IV, V). Drawn from a photograph.

present there and has since been reacted away or broken off.

Friable rim

The outer portion of HAL consists of a thick (up to 2 mm) and very friable, fine-grained rim sequence. The rim is unusual and complex in mineralogy and texture and shows little resemblance to the much thinner rims on Type A and B inclusions described by WARK and LOVERING (1977). Phases so far encountered are both refractory and volatile-rich: perovskite, nepheline, sodalite, Ca–Mg–Fe–Al-pyroxene, Ca-phosphate, hibonite, grossular, andradite, Al–Fe-oxide, Ti–Fe-oxide, Ti–Sc–Zr-oxide, olivine, pentlandite and Ni–Fe metal.

Five distinct layers within the friable rim can be distinguished on the basis of mineralogy. The thickness of each layer, the constituent minerals and their approximate relative abundances in each layer from I (interior) to V (exterior) are given in Fig. 6. Layers I–IV have an aggregate thickness of 90–450 μm. They are poor in dark colored minerals and are seen in Fig. 1 as a light zone enveloping the interior hibonite grains and black rim. Layer V, in contrast, is richer in dark colored minerals and displays prominent light/dark banding in places (Fig. 1). The beginning of layer V is marked by the innermost, continuous dark band.

Layer I. This, the innermost layer of the friable rim, is discontinuous around the inclusion. Where present, it has an abrupt contact with the black rim and a fairly sharp contact with rim layer II marked mainly by the appearance of abundant perovskite (Fig. 2). Layer I consists predominantly of nepheline and sodalite in a 2:1 ratio, with minor anorthite, Ti–Fe-oxide and an Al–Fe-oxide. The nepheline and sodalite occur intergrown in fairly compact masses of indeterminate grain size with about 5% void space and have inclusions of fine, elongate (<2 μm long) grains of Ti–Fe-oxide.

Layer II. This, as well as layers III–V, is laterally continuous in the two thin sections of rim material and is probably continuous around the entire inclusion. The difference between layer II and layer I is the presence in the former of abundant (~10–15%) perovskite, plus grossular, andradite and pyroxene.

The perovskite occurs as subhedral to rounded grains, 1–10 μm in size (Fig. 7). It and the Ti–Fe-oxide are partially or completely enclosed poikilitically in fractured nepheline and subordinate sodalite, suggesting the latter two minerals, both volatile-rich, crystallized later. Grossular, andradite and pyroxene occur as irregularly-shaped and fractured masses up to 20 μm in size. Grossular poikilitically encloses perovskite and is itself enclosed by nepheline, indicating the formation sequence perovskite, grossu-

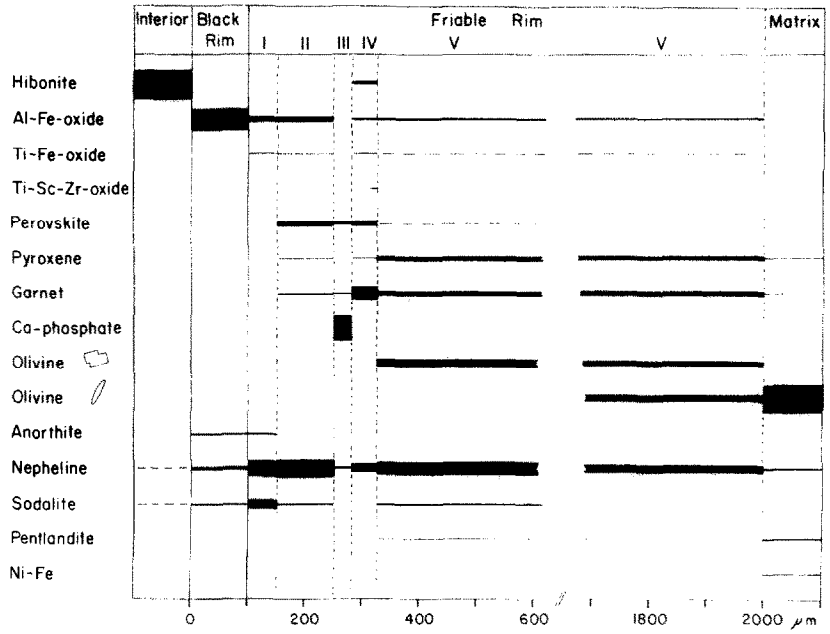

Fig. 6. Distribution and relative abundances of minerals in HAL.

lar, nepheline. The positions of andradite and pyroxene in the crystallization sequence are not clear in this layer.

The Al–Fe-oxide is chemically and optically similar to the material making up the bulk of the black rim. It occurs as masses up to 45 μm in size, (Fig. 8), each of which shows homogeneous extinction in polarized light indicating they are single crystals. The masses appear to be corroded and replaced by nepheline around their margins and also in their interiors where nepheline forms series of parallel streaks across their surfaces, presumably following a structural weakness in the Al–Fe-oxide.

Where layer I is missing, the contact between the black, compact rim and layer II is gradational. In this region, abundant perovskite is embedded in a fine-grained mixture of Al–Fe-oxide, nepheline and sodalite in association with elongated crystals of anorthite, up to 10 μm long.

Layer III. Layer III contains ~85% Ca-phosphate (possibly hydroxy-apatite), 10% perovskite and the remainder nepheline, grossular-andradite intergrowths, pyroxene and Ti–Fe-oxide. The phosphate grains have a wide range of size, are highly irregular in shape and give layer III a somewhat clastic appearance (Fig. 9). Textural relationships with other minerals are not clear and give no clue as to crystallization sequence.

Layer IV. A remarkable variety of both refractory and volatile-rich minerals occurs in rim layer IV. As well as most of the minerals found in layers II and III (exclusive of Ca-phosphate and sodalite), layer IV contains hibonite and a Ti–Sc–Zr-oxide. Hibonite is present as subrounded to very elongated grains up to 30 μm in size. Its occurrence is somewhat sporadic, tending to occur in clusters in only a few regions of the layer. The Ti–Sc–Zr-oxide is rare. Only five grains were found in one small area abutting layer V. The grains are tiny (1–5 μm) and some are intergrown with perovskite. Grossular and andradite are invariably intergrown with one another in composite masses up to about 20 μm in size (Fig. 9). Rimming relationships suggest the following order of mineral formation: perovskite, grossular and andradite, nepheline. Hibonite, Ti–Sc–Zr-oxide and Ti–Fe-oxide all formed before nepheline.

Layer V. Minerals found in layer V but not in the other layers are olivine, pentlandite and Ni–Fe metal. Refractory phases such as hibonite and Ti–Sc–Zr-oxide are absent. About 30% of this layer consists of a mineral with the composition of olivine Fa_{22-34}. However, it has an unusual habit with rectangular cross-sections (Fig. 10), distinctively different from olivine in the Allende matrix which has a barrel-shaped or platey form (Fig. 11). Grain rims are enriched in iron relative to cores. The mineral is speckled with very fine (0.1 μm) Al-rich material (Fig. 12), possibly also containing Fe, of unknown origin. Grossular-andradite intergrowths and pyroxene form separate, irregularly-shaped masses of widely ranging size up to 100 μm, considerably larger than masses of these minerals in the other rim layers. Olivines, garnets and pyroxenes are enclosed in a matrix of highly fractured and porous nepheline and sodalite (Fig. 10) such as is found in layers I, II and IV of the friable rim. In other places, olivines, garnets and pyroxenes, some rimmed by feldspathoids, form a porous aggregate of angular grains, resembling a sedimentary rock (Fig. 13).

A part of layer V (Fig. 1, left) displays well-developed, alternating, light and dark banding. The dark bands are rich in masses of pyroxene and garnet; the light ones rich in olivine. This is strongly suggestive of accretionary, rhythmic layering. The bands are undulose and concentric and vary laterally in thickness. The amplitudes of concentric irregularities increase toward the outside of layer V. That no band has parallel margins indicates that the irregularities cannot be folds caused by the forcible impression of adjacent inclusions (Fig. 1, upper left) into internally rigid bands. Of the bands observed in the left portion of Fig. 1, only the innermost is continuous around the inclusion. Elsewhere, the banding is indistinct or absent. Where observed, however, it is highly irregular and contorted (Fig. 1, lower middle), perhaps indicating disruption during accretion due to small particle impact.

The contact of rim layer V with the matrix of Allende is gradational. Barrel-shaped olivine and pentlandite, minerals typical of the matrix, begin to appear ~900 μm from the contact with rim layer IV. Garnet, nepheline and rectangular olivine, phases characteristic of rim layer V, per-

Fig. 2. SEM image of HAL in a polished thin section, showing hibonite (H), black rim (BR), friable rim layers I–IV and the inner part of layer V.

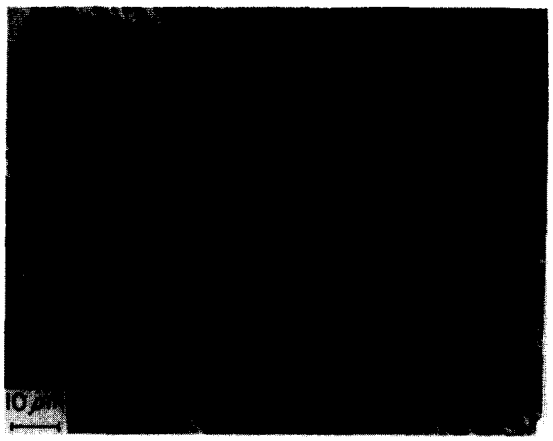

Fig. 5. High-contrast SEM image of black rim. Mottled and feathery textures are due to mixtures of Al–Fe-oxide, nepheline, sodalite and anorthite in varying proportions, and may result from devitrification of a glass.

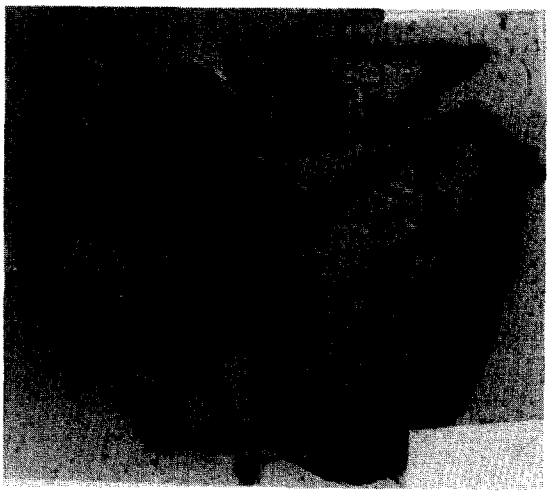

Fig. 3. Hibonite crystal showing exsolved needles (upper left) and secondary phases deposited on its surface (patchy material on right). Composition profile A–B is shown in Fig. 14. Transmitted light. Crystal is 700 μm wide.

Fig. 7. Friable rim layer II, showing grains of perovskite (P) and Ti–Fe-oxide (T) partially enclosed by a matrix of porous and fractured grossular and andradite garnet (G) and nepheline (N).

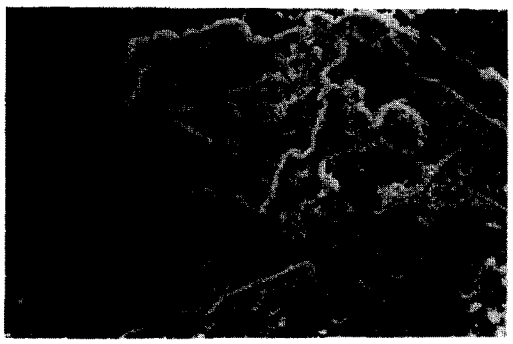

Fig. 4. Pits and secondary alkali-rich phases on hibonite. Width of field is 200 μm. At higher magnification, pits are hexagonal in shape.

Fig. 8. A large single crystal of Al–Fe-oxide (A) in rim layer II, showing replacement by nepheline both as irregular patches (N) and as many fine blebs oriented NW–SE. Large bright spots in the crystal are artifacts due to electron beam burn-off of the conducting film.

Fig. 9. Rim layer III (center, running N–S) consists mostly of Ca-phosphate (CP). Layer II (right) shows nepheline and perovskite; layer IV (left) shows perovskite, garnet and nepheline.

Fig. 11. Allende matrix near HAL, showing olivine with barrel-shaped sections and pentlandite (Pe) and nickel–iron metal (M).

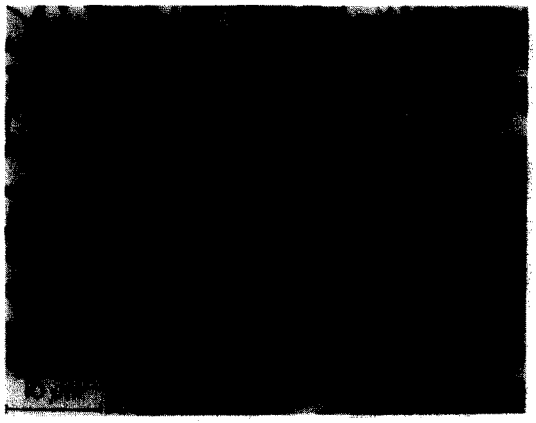

Fig. 10. Rim layer V, inner portion. Blocky, olivine-like phase (Ol), pyroxene (Px) and garnet in a matrix of nepheline and dusty Al–Fe-oxide.

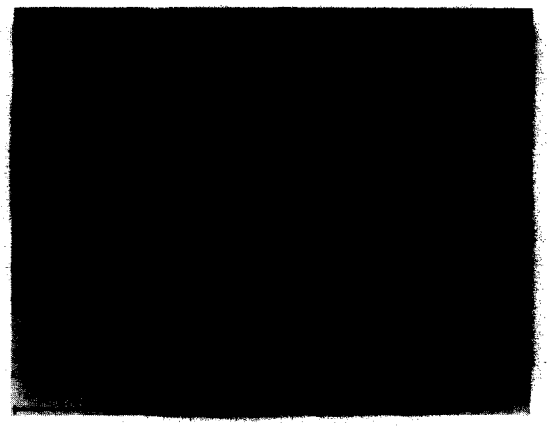

Fig. 12. Blocky, rectangular olivine in layer V. Small dark inclusions are Al-rich material.

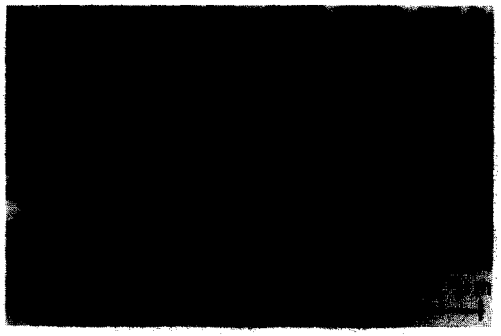

Fig. 13. Rim layer V exterior to portion in Fig. 10. Olivine (light grey) and nepheline (dark grey).

Table 1. Compositions (mean and range) of hibonite crystals in the Allende inclusion HAL (wt %)

	Interior crystals 19 analyses	Rim grains 4 analyses
MgO	<0.01	0.40 (0.25- 0.59)
Al_2O_3	89.95 (88.07-91.00)	88.09 (87.08-88.58)
SiO_2	<0.02 (<0.02- 0.04)	0.14 (0.07- 0.26)
CaO	8.71 (8.32- 9.02)	7.92 (7.79- 8.06)
Sc_2O_3	0.05 (<0.03- 0.09)	0.33 (0.24- 0.44)
TiO_2	0.71 (0.60- 1.06)	1.64 (1.37- 2.01)
V_2O_3	<0.02	<0.02
Cr_2O_3	<0.02	<0.02
FeO	0.32 (0.20- 0.43)	0.80 (0.68- 0.90)
Y_2O_3	<0.03	<0.03 (<0.03- 0.05)
ZrO_2	<0.02 (<0.02- 0.03)	0.08 (<0.03- 0.13)
Total	99.74	99.40
	Cations per 38 oxygen atoms	
Mg	------	0.134
Al	23.732	23.381
Si	------	0.032
Ca	2.089	1.911
Sc	0.010	0.065
Ti	0.120	0.278
Fe	0.060	0.151
Zr	------	0.009
Σ	26.011	25.961

sist at high concentrations for another 800 μm beyond this point.

MINERAL CHEMISTRY

Hibonite

Hibonite occurs primarily as large crystals in the interior of the inclusion, but also as tiny needles and sub-rounded crystals in rim layer IV.

The hibonite in the interior of HAL is remarkably pure, containing >99 mol % of the model hibonite molecule, $CaAl_{12}O_{19}$, and only minor amounts of other components (Table 1). Si, V, Cr and Y in the interior hibonites are all below the detection limit of 0.02% of the oxide (0.03% for Y_2O_3). It is the purest hibonite of analyses reported in the literature to date and is unique among others analyzed in having MgO less than 100 ppm (the detection limit in electron microprobe analyses). In contrast, hibonites described in KEIL and FUCHS (1971) and ALLEN *et al.* (1978) contain 0.2–4.6% MgO.

The exsolved needles of a Ti-rich phase in the hibonite imply that the crystal structure of the hibonite was once richer in Ti than it now is. The problem is that the residual TiO_2 content (0.60–1.06%) of the hibonite in equilibrium with the exsolved phase is much lower than that of other Allende hibonites (as high as 8.5%) which show no evidence for exsolution of titanian phases. What peculiarity of HAL's history caused the Ti content of its hibonite to be restricted to a value lower than that of most other Allende hibonites? Perhaps hibonite in HAL cooled more slowly than the others. Another possibility is that the Ti in HAL hibonite may have a different valence from that in the others, but this can be ruled out on the basis of the following considerations. ALLEN *et al.* (1978) presented a convincing case that the bulk of the Ti in normal Allende hibonites is present as Ti^{4+}, its highest oxidation state, based on graphs of Ti vs Mg and Ti + Mg vs Al cations in formulae calculated from hibonite analyses. Large negative Ce anomalies in HAL hibonite (TANAKA *et al.*, 1979) show that it formed under more oxidizing conditions than normal Allende inclusions. Thus, Ti in HAL hibonite must also be present as Ti^{4+}.

In the normal hibonites, Ti^{4+} couples with a divalent cation, usually Mg^{2+}, to substitute for 2 Al^{3+}. Table 1 shows that, even though Mg^{2+} is very low in HAL hibonite, the ratio of Ti to divalent cations is actually <1, assuming all the Fe is divalent and including excess Ca. It is possible that the exsolved Ti^{4+} was originally coupled with Fe^{2+}. Although other Allende hibonites also contain significant Fe^{2+}, the difference between those and HAL may be that HAL was later subjected to so oxidizing an environment that some of its Fe^{2+} was converted to Fe^{3+}, causing one Ti^{4+} to exsolve for every 4 Fe^{2+} oxidized. Perhaps the exsolution in HAL was simply caused by the replacement of 3 Ti^{4+} and a vacant octahedral site by 4 Al^{3+} and this did not happen in other hibonites because they were unable to exchange with so Al-rich a source. Another possibility is that

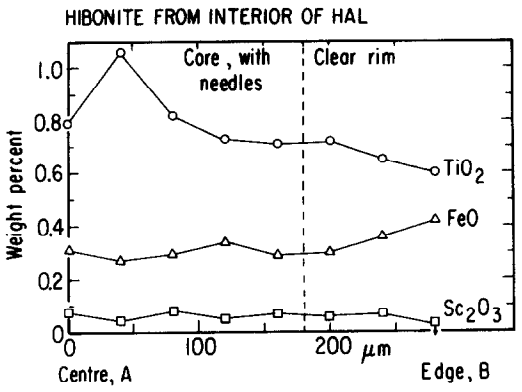

Fig. 14. Zoning profile in hibonite of Fig. 3.

HAL hibonite formed more rapidly and/or at a higher temperature and/or from a system with a higher Ti/divalent cation ratio than other Allende hibonites such that it originally crystallized with Ti^{4+} and O^{2-} in structural vacancies. At lower temperature, the structure could no longer tolerate this excess TiO_2 and it exsolved.

In the single hibonite flake shown in Fig. 3, Fe increases and Sc and Ti decrease toward the rim within the clear, needle-free, outermost 80 μm (Fig. 14). Assuming that these elements are present in the hibonite crystal structure rather than in inclusions, the hibonite is chemically zoned in a sense opposite to that expected had the Sc and Ti been withdrawn from the rim and incorporated by the exsolved needles. We conclude that the zoning directions of all the elements in the clear rim are unaffected by exsolution of the needles. Either the hibonite grew outwards with falling temperature, incorporating more and more FeO and less and less Sc_2O_3 and TiO_2 from the medium in which it crystallized or an originally homogeneous crystal partially re-equilibrated its rim after growth.

Compared to the large interior hibonites, the small hibonite crystals in rim layer IV are richer in both refractory and non-refractory trace and minor elements. Enrichment factors for Zr, Sc, Ti, Fe, Si and Mg are ≥4, 6.6, 2.3, 2.5, ≥7.0 and ≥40, respectively, in rim hibonites compared to the mean value for interior ones. Nevertheless, even the exterior hibonites are poorer in MgO (0.25–0.59%) than most of those reported in the literature.

Perovskite

Perovskite is close to pure $CaTiO_3$ in composition, except for small amounts of Zr, Y and Sc (Table 2). Cr

Table 2. Minor elements in three perovskite grains in the rim of Allende inclusion HAL (wt %)

Sc_2O_3	0.09	0.10	0.14
Cr_2O_3	<0.07	<0.07	<0.07
Y_2O_3	0.09	0.10	0.08
ZrO_2	0.58	0.64	0.83

Table 3. Analysis of Ca-phosphate in Allende inclusion HAL

	Weight %	P and Ca ions per 25 oxygen atoms	
Na_2O	<0.01	P	6.075
MgO	0.02	Ca	9.812
Al_2O_3	0.16	Ca/P**	5:3.10
SiO_2	0.31		
P_2O_5	42.04		
CaO	53.65		
MnO	<0.03		
FeO	0.77		
Cl	0.19		
F	<0.20		
-O=Cl	0.04		
Total	97.50*		

* Includes Sc_2O_3 of 0.4%, determined semiquantitatively.

** This ratio for apatite = 5:3.00; for whitlockite = 5:3.33.

was not detected. Refractory lithophiles are strongly enriched and highly fractionated from one another relative to Cl chondrites. Zr, Y and Sc have mean enrichment factors of 1627, 446 and 113, respectively. Ce (≤60 ppm) and Nd (≤50 ppm) were looked for, but not detected.

Sc–Ti–Zr-Oxide

A pure analysis of this mineral is not possible because of its fine grain size and intergrowths with perovskite. Correction for the contribution of adjacent material to the analyses is further complicated by the variety of surrounding minerals. Microprobe analyses with all elements considered as oxides sum close to 100%, indicating the mineral is an oxide. The atomic ratio Ti:Sc:Zr is estimated to be about 10:7:3. The only other reported Sc phase in a meteorite is an Sc-silicate from a Fremdling in Allende (EL GORESY *et al.*, 1978). The present phase is apparently a new mineral. Its presence in this inclusion, albeit minor in abundance, reflects the highly refractory nature of this inclusion (TANAKA *et al.*, 1979).

Ca-Phosphate

The fine grain size of the phosphate and admixture of other phases complicates its analysis. The purest analysis is given in Table 3. Minor elements detected, Fe, Si, Al and Mg, are not necessarily in the phosphate but may arise from excitation of adjacent phases by the microprobe electron beam.

The Ca:P ratio is close to 5:3, compatible with a carbonate-free apatite and not with whitlockite, where this ratio ideally is 3:2. Chlorine is minor (0.19%) and fluorine was not detected (<0.20%). Thus, the phase must be hydroxy-apatite. This interpretation is compatible with the low total (97%), 1.9% H_2O being present in this phase. Alternatively, the phase could

Table 4. Compositions of Al–Fe-rich material (wt %)

	Black rim			Layer II		
	1	2	3	4[a]	5[a]	6[a]
Na_2O	2.14	2.22	3.75	0.98	2.36	2.75
MgO	0.30	0.15	0.22	6.88	5.00	3.31
Al_2O_3	59.03	55.52	50.32	65.54	68.49	68.54
SiO_2	6.37	12.40	18.23	2.02	4.17	7.52
K_2O	0.07	0.03	0.21	----	----	----
CaO	2.55	4.03	3.83	0.39	0.54	1.66
Sc_2O_3	<0.03	<0.04	<0.04	----	----	----
TiO_2	0.36	0.67	0.62	----	----	0.46
V_2O_3	<0.02	<0.02	<0.02	----	----	----
Cr_2O_3	<0.02	0.03	<0.02	----	----	----
MnO	0.16	n.d.	0.13	----	----	----
FeO	29.37	23.14	23.75	23.24	18.98	13.76
Y_2O_3	<0.04	<0.06	<0.04	----	----	----
ZrO_2	<0.03	<0.04	<0.03	----	----	----
Total	100.35	98.19	101.10	99.90[b]	100.43[c]	98.55[d]
	Cations per 12 oxygen atoms					
Na	0.337	0.344	0.564	0.150	0.352	0.405
Mg	0.036	0.018	0.025	0.812	0.573	0.375
Al	5.656	5.234	4.605	6.114	6.207	6.143
Si	0.518	0.992	1.415	0.160	0.321	0.572
K	0.007	0.003	0.021	-----	-----	-----
Ca	0.222	0.345	0.318	0.033	0.045	0.135
Sc	-----	-----	0.002	-----	-----	-----
Ti	0.022	0.041	0.036	-----	-----	0.026
Cr	-----	0.002	-----	-----	-----	-----
Mn	0.011	n.d.	0.008	-----	-----	-----
Fe	1.997	1.548	1.542	1.538	1.220	0.875

[a] Energy dispersive analyses.
[b] Includes 0.37 CoO, 0.48 ZnO.
[c] Includes 0.31 Cl, 0.58 ZnO.
[d] Includes 0.55 Cl.
n.d.–Not determined.
-----–Not detected.

be a previously unknown volatile-free phosphate, the low total a consequence of its fine grain size.

Ce ($\leq$60 ppm) and Nd ($\leq$50 ppm) were looked for, but not detected. Semiquantitative analyses give Sc_2O_3 up to 0.4%.

Al–Fe-Oxide

An Al–Fe-oxide makes up the bulk of the black rim and is found as small patches in all layers of the friable rim. The oxide is extensively altered to very fine-grained nepheline, sodalite and anorthite and, as a result, microprobe analyses always reflect the presence of significant proportions of these phases. The volatile-rich nature of the bulk material, Al–Fe-oxide plus alteration products, is shown by the presence of Na, K, Mn, Cr, Co, Zn and Cl in the analyses in Table 4. Refractory lithophiles Sc, Zr and Y could not be detected. To obtain the composition of the Al–Fe-oxide itself, it is necessary to correct for the presence of the alteration products. Using Na, Cl and Si concentrations to correct for nepheline (~15–30%), sodalite (~0–8%) and anorthite (~0–12%), respectively, gives residual compositions dominated by Al and Fe for the oxide in the black rim and Al, Fe and Mg for that in the friable rim, with only minor amounts of other cations. The residual compositions from 23 analyses adjusted in this manner have the molar ratio $Al_2O_3/Al_2O_3 + FeO + MgO$ of 0.49–0.69 with a mean of 0.55. The oxide therefore has an excess of Al over that present in stoichiometric hercynite spinel ($FeAl_2O_4$) where this ratio is 0.5.

X-ray powder patterns of two grains picked from the black rim were generously obtained for us by Professor P. B. Moore. As well as strong lines due to sodalite and weak lines to nepheline, they both show all the major lines of spinel, many of which are broad and fuzzy. The strong linear features in the oxide observed in thin section, whether inclusions, alteration products or cleavage traces and the moderate birefringence of the oxide indicate that it is not cubic

and therefore cannot be a non-stoichiometric spinel, the latter being cubic and isotropic (PEDERSON, 1978). The broadness of the reflections and paucity of lines obtained in our patterns, even after long exposure times, prohibits determination of the structure.

Garnets

Grossular and andradite each contain a small proportion of the pyrope component and up to 0.03% Sc_2O_3. As in other Allende inclusions, intermediate compositions in the range $Gross_{90}And_{10}$ to $Gross_1And_{99}$ are not present in HAL in spite of the coexistence of the nearly pure end-members. This problem is brought into sharp focus in rim layers II–V. Here are found intergrowths of the two garnets, in composite masses reaching 20 μm in size in layer IV. It is difficult to invoke exsolution to explain this coexistence because the excess free energy of mixing of these two components is slightly negative (GANGULY, 1976). Thus, not only do they form a nearly ideal solution with one another, but also what deviations from ideality do exist are in the direction of making mutual solid solutions more stable than ideal ones, rather than in the direction of unmixing. In addition, a continuous series of garnet compositions between grossular and andradite is known from terrestrial occurrences and no exsolution textures have been reported. Perhaps the intergrowths in rim layer IV were once intergrowths of one garnet with another phase which was subsequently replaced by the other garnet. The compositions of the coexisting garnets pose a problem for this model, however, as it is difficult to see how an inclusion in grossular could be replaced by pure andradite without adding any more than 10 mol % andradite to the host or how grossular could replace an inclusion in andradite while adding only 1 mol % grossular to the host. Another possibility is that the intergrowths are mechanical mixtures of clumps of very fine grains of one garnet embedded in a matrix of very fine grains of the other garnet, although the compact nature of the clumps would argue against this. This model would have the advantage, however, that the two garnets could have formed in separate locations and could have mixed together later, at temperatures low enough to prevent significant reaction between them.

Other minerals

Described briefly here are pyroxene, olivine and nepheline. Analyses were performed by energy-dispersive methods.

Pyroxenes are exclusively Ca–Mg–Fe types, varying from Fe-salite to hedenbergite in composition. They are low in Al_2O_3 (up to 1.8%) with the higher values in the more Mg-rich pyroxenes, and contain no detectable TiO_2. They are similar to pyroxenes in the outer zones of rims on Type A and B inclusions (WARK and LOVERING, 1977; ALLEN *et al.*, 1978).

The phase in rim layer V whose composition resembles olivine and whose crystals are rectangular in cross-section contains finely-disseminated Al-rich material. The latter makes it impossible to obtain an analysis of the olivine-like material which is free of Al_2O_3. Table 5 shows the lowest-Al_2O_3 analysis of this phase which we were able to obtain. From this, the closeness to olivine stoichiometry is clear. On this basis, we will assume that the phase is indeed olivine, despite the absence of confirmatory X-ray data. Its composition is in the range Fa_{22-34}, less iron-rich than that in the Allende matrix ($\sim Fa_{50}$), more iron-rich than in chondrules (Fa_{0-20}) and overlapping with the range in amoeboid olivine aggregates (Fa_{1-36}). The olivine composition in this inclusion is thus distinctive and not the same as that encountered elsewhere in Allende.

Nepheline is Ca-rich (2.3–2.8% CaO) and contains 1.4–1.7% K_2O. Compositions are very similar to those in a Type A inclusion described by ALLEN *et al.* (1978) and in amoeboid olivine aggregates (GROSSMAN and STEELE, 1976).

DISCUSSION

It is a formidable task to pose models for HAL's origin which are consistent with all the available mineralogical and isotopic data. On the one hand, HAL's core consists of hibonite, the first major phase to condense from a cooling gas of solar composition; yet, it contains no excess ^{26}Mg. On the other hand, HAL's friable rim contains some phases which, if they formed in a gas of solar composition at all, must have done so at vastly lower temperatures than the hibonite. Nonetheless, LEE *et al.* (1979) demonstrated that both core and rim are *isotopically* related, in that samples of both materials are devoid of excess ^{26}Mg and have identical, anomalous Ca isotopic compositions. They showed that Ca in core hibonite, black rim and inner layers of the friable rim suffered extreme mass-dependent isotopic fractionation and contains components with distinct nucleosynthetic histories, while Mg in the same samples has normal isotopic composition, showing no effects due to fractionation, ^{26}Al decay or nebular heterogeneity. Based on these constraints and the mineralogical information then available, LEE *et al.* (1979) suggested that HAL condensed from a reservoir containing abnormal abundances of Ca isotopes and possibly also ^{26}Al

Table 5. Composition of the olivine-like phase with rectangular cross-sections in rim layer V

	Weight %		Atomic Proportions per 4 oxygen atoms
SiO_2	38.1	Si	0.974
Al_2O_3	2.3	Al	0.070
TiO_2	0.2	Ti	0.003
FeO	19.7	Fe	0.421
MnO	0.2	Mn	0.004
MgO	39.3	Mg	1.497
CaO	0.3	Ca	0.008
Na_2O	0.4	Na	0.020
Total	100.5		

from a special nucleosynthetic source. Later, it was heated so intensely that most of its original Mg was evaporated away, including ^{26}Mg from ^{26}Al decay, as well as ~50% of its Ca, producing the observed Ca isotopic mass fractionation in which heavy isotopes are enriched in HAL relative to light ones. Finally, those workers pictured that the hibonite core and possibly other surrounding phases produced in this way underwent thorough reaction with a surrounding Ca-poor gas to produce the rim layers. In this process, normal Mg was introduced and the pre-existing Ca isotopic anomalies were preserved.

ALLEN *et al.* (1979) proposed an alternative model in which both the rim minerals and possibly also the hibonite condensed directly from a vapor and the rim phases accreted, grain-by-grain, around the hibonite core. This model would require the core and rim phases to have originated in the same, low-^{26}Al, gaseous reservoir in which the Ca isotopic composition had been previously modified by additions from exotic sources and by mass fractionation processes.

The remainder of this paper will be devoted to a discussion of the physico-chemical conditions under which HAL formed in light of the petrographic and electron microprobe observations described above. From these, we will attempt to choose between the formation models which have so far been proposed for HAL.

History of the hibonite

It is difficult to tell whether the euhedral hibonite crystals in the core of HAL condensed directly from a vapor or crystallized from a melt. The euhedral feldspathoid crystals on the hibonite surfaces certainly indicate that the hibonite crystals, after they formed, reacted with a vapor phase from which alkalis were deposited. The same vapor phase alteration process may have been responsible for etching the hibonite, thereby producing the hexagonal pits on its surfaces. Although data for hibonite are not available, experimental studies with Al_2O_3 have shown that acid etching can produce surface pits (MCVICKERS *et al.*, 1962), whereas growth of Al_2O_3 from a vapor gives rise to isolated surface hills without pits (MINAGAWA *et al.*, 1968). The FeO concentration profile in the hibonite shows a slight upturn toward the edge of the clear rim which may be due to a secondary process or a change of conditions during a primary one. The FeO may have been deposited during the process that created the feldspathoids or it may have diffused into the hibonite from the black rim. Nevertheless, the fact that the profile flattens to a non-zero FeO concentration within the hibonite core suggests that there was a prior stage of FeO incorporation by the hibonite, either during primary growth or during an earlier secondary process than that which affected its rim.

History of the black rim

The black, compact rim surrounding the hibonite core was once molten. It apparently quenched to an Al-rich glass which partially devitrified to form a non-stoichiometric spinel-like phase. During or after that event, it reacted with a medium from which alkalis were introduced to form feldspathoids which occur as cross-cutting veinlets and replace devitrification textures in the black rim. This was probably the same vapor phase alteration process which deposited feldspathoids on the interior hibonite crystals.

The critical observation is that the black rim corrodes the edges of the hibonite crystals. If the hibonite crystallized from a melt related to that which formed the black rim, then the liquid must have undergone a wholesale change in composition, perhaps by reaction with a surrounding gas, after hibonite crystallization and prior to quenching. In this case, the original liquid may have been a primary condensate or a secondary liquid, formed by the melting of solid condensate aggregates in the nebula. If the hibonite did not crystallize from such a melt, three possibilities arise. The hibonite crystals could be primary solid condensates which were originally coated by other solid condensates. These mixtures could have been partially melted around the edges of the hibonite crystals and then quenched, producing the corrosion textures. Or, the original hibonite could have reacted with the gas to produce a liquid condensate which quenched to form the black rim. The final possibility is that the hibonite collided with a liquid droplet which was not in equilibrium with it and the liquid froze to form the black rim.

Let us first examine the compatibility of each of these alternatives with the LEE *et al.* (1979) model. In this model, it is difficult to see how the hibonite crystals present in HAL today could be the original crystallization products from a primary condensate liquid, the first of the above possibilities. This is because a partial vaporization event intense enough to drive off all the Mg and 50% of the Ca must be postulated to have taken place after primary condensation. It is very unlikely that the original crystals, which now contain 8.71% CaO, would be preserved during such a process. Similarly, the above scenario in which mixtures of primary condensate hibonite and other phases were melted around the hibonite crystal margins is not compatible with this model because the hibonite cores would have to be preserved intact during this or a later partial vaporization event. In the case in which hibonite crystallized from a melt which was a consequence of the same secondary heating event as the partial vaporization, the black rim would have been the precursor that reacted with the gas to form the friable rim in this model. This is also an unlikely alternative because, even though the black rim was never continuous around the hibonite core, the friable rim surrounds the inclusion completely. The same observation argues against the possibility that the black rim formed when a liquid droplet collided with the hibonite and then froze if the LEE *et al.* (1979) model for the origin of the friable rim is

adopted. Finally, had the hibonite, floating freely in the gas, reacted with it to form a condensate liquid, one would expect the reaction product to surround the core on all sides, which is clearly not the case. Thus, the LEE *et al.* (1979) model is difficult to reconcile with each of the possibilities for the origin of the black rim mentioned above.

In the model of ALLEN *et al.* (1979), the phases in the friable rim are not replacement products and the interpretation that the black rim never completely surrounded the hibonite core constrains the various alternatives posed for the origin of the black rim. For the same reason mentioned in the previous paragraph, reaction of the hibonite to form a condensate liquid can be ruled out. Hibonite crystallization from either a primary or secondary melt which later became the black rim could have occurred in this model, however, if the amount of melt remaining after hibonite crystallization was so small that its distribution around the hibonite was discontinuous. Formation of the black rim by melting of a mixture of hibonite and adjacent grains is another viable scenario in the ALLEN *et al.* (1979) model, since the melt need not have formed all the way around the hibonite if the other grains had only accreted in certain places. Finally, the hibonite-droplet collision possibility is also compatible with the ALLEN *et al.* (1979) model.

History of the friable rim

LEE *et al.* (1979) proposed that the friable rim formed during reactions between pre-rim material and a nebular gas phase. In such a model, production of the observed series of concentric layers is in many ways analogous to the formation of a sequence of mineralogically-distinct zones at the boundary between a fluid-charged hydrothermal vein and a pre-existing wall rock during metasomatism. In such instances, mineralogical and chemical zonation are due to a number of factors, including the establishment of chemical potential gradients perpendicular to the contact surface, modification of these gradients as the fluid phase emanating from the vein changes its composition during passage through and reaction with the adjacent rock, the temperature gradient across the contact and the differing diffusion rates of different chemical species. In the present case, however, the gaseous reservoir is probably so much more massive than HAL and other nodules like it that it can be considered infinite and its change in composition with progressive reaction can be ignored. Also, because HAL is so small, the temperature gradient across it was probably negligible. It thus seems clear that, if the friable rim formed by reaction, then the mineralogical zonation was controlled by diffusion processes along radial chemical potential gradients and may have also been influenced by temporal changes in temperature, pressure and composition of the surrounding gas. Under such conditions, the same sequence of zones would be expected to have formed all the way around the inclusion unless some initial chemical differences or physical barriers to some or all of the ions existed along some radiants. Even in the case where such complications might fortuitously act to cause the omission of a particular mineralogical zone along a particular radiant, significant changes in the mineralogical and chemical compositions of adjacent zones would be expected along the same radiant relative to their usual compositions in other sectors. In the case of HAL, rim layer I pinches out in certain regions and the typical mineral assemblage of rim layer II merges with the black rim directly. In this contact region, the phases typical of rim layer II are embedded in a mixture of Al–Fe-oxide, nepheline and sodalite similar to that in the black rim. In this mixture, the abundances of feldspathoids are enhanced relative to those in the black rim and anorthite, whose occurrence is restricted to veins elsewhere in the black rim, is present as intergrown needles. What is missing is rim layer I: a layer of feldspathoids with minor Al–Fe-oxide, sandwiched between the razor-sharp boundary that separates it from the black rim on one side and the abundant perovskite which marks rim layer II on the other side. Compared to other areas around HAL, no mineralogical differences are evident in the rims adjacent to this contact region. From what has been said above, we consider these observations to constitute a powerful argument against the reaction model. The argument is only valid, however, if mechanical deformation after rim formation is not the cause of the absence of rim layer I, although it is not clear how such a process could be selective for only one rim layer.

The mineralogical and textural character of rim layer V also argues against the reaction model. The rhythmic banding seen in this layer is difficult to explain in such a model, but is readily understandable in an accretion model in which HAL was cycled alternately between a region rich in olivine and one rich in garnet and pyroxene. Toward the outside of rim layer V are found barrel-shaped olivine crystals, metallic nickel–iron and pentlandite, phases identical with those typical of the matrix of the Allende meteorite and which are not found elsewhere in HAL's friable rim. In view of the mechanical disruption of parts of the friable rim discussed above, squeezing of these minerals into HAL after incorporation into the Allende parent body has to be considered as a possibility. The arguments against this, however, are that these phases are completely surrounded by minerals typical of the inner part of rim layer V, no trails of these phases could be traced outward to the matrix and their occurrence persists for $\sim 900\,\mu m$ into the friable rim, or nearly 50% of the radius of the entire rim sequence. There are only two ways remaining to account for their presence in rim layer V if the reaction model is correct. Either they represent remnants of the original, pre-rim mineral assemblage or they are products of the reaction between such material and the surrounding gas. The first possibility is ruled out by the fact that these minerals show no reaction

relationships with other phases in rim layer V. They look no different from their unaltered counterparts in the Allende matrix. If it is assumed that each rim layer in the reaction model is an equilibrium assemblage, the second possibility can be ruled out by the coexistence in rim layer V of andradite, containing ferric iron, and metallic nickel–iron. It also seems highly unlikely that two different olivine crystal morphologies would result from the same reaction. It appears, instead, that the two types of olivine crystals in rim layer V grew under different physico-chemical conditions and are not genetically related to one another.

We note that, although the petrographic data strongly suggest a 'sedimentary' origin for the friable rim, they cannot rule out the possibility that HAL's constituent grains may be volatilization residues. Thus, one class of model with the potential of satisfying both the petrographic information outlined here and the isotopic constraints (LEE *et al.*, 1979) would involve starting with an assemblage of presolar grains having nucleosynthetic Ca isotope anomalies, partial volatilization producing mass-fractionated Ca, recondensation of some of the gas so produced and accretion of mixtures of these grains to form the friable rim around the hibonite core. This type of model has a whole series of problems of its own. Most of our objections to such models are based on chemical data for HAL which will be discussed in a later paper.

We prefer a model for the origin of the friable rim similar to that proposed by ALLEN *et al.* (1979) in which each rim layer formed by the accretion of grains of a distinct suite of condensate minerals. After assembly of an originally highly porous rim sequence, HAL underwent vapor phase reactions leading to the deposition of feldspathoids throughout the friable rim and the black rim and even on the surfaces of the interior hibonite crystals.

Because most of the material presently in rim layer I is feldspathoids, it is difficult to reconstruct its primary condensate mineralogy. The only other phases present are the Al–Fe-oxide and a Ti–Fe-oxide. Perhaps Al-rich liquid droplets were common in the region of the nebula where HAL originated and formed in the same way as the Al-rich liquid that pre-dated the black rim, i.e. by condensation of a primary liquid or by secondary melting of mixtures of solid condensates. If such droplets were so small that they quenched to glasses prior to hibonite crystallization, an Al–Fe-oxide similar to that which formed in the black rim could have been produced during devitrification of these glasses as well. Such grains or their fragments may have accreted around the black rim of HAL together with grains of the Ti–Fe-oxide. It is impossible to condense an Al–Fe-oxide liquid from a gas of solar composition under equilibrium conditions. This is also highly unlikely under non-equilibrium conditions as gaseous Al would have to be undercooled by 1000 K in order for it to condense under conditions where oxidized iron is stable. A gas far more oxidizing than one of solar composition is indicated, so that oxidized iron could condense at the same high temperature as Al_2O_3. Such conditions could also give rise to the Ti–Fe-oxide. If these were secondary liquids, formed by melting mixtures of solid condensates, a similar conclusion about the oxidizing nature of the gas is reached as it would only be under such conditions where pre-liquid mixtures rich in FeO and Al_2O_3 and poor in other elements would be likely. As mentioned above, the hibonite crystals in the core of HAL may have formed from a primary or secondary melt similar to those which may have given rise to the Al–Fe-oxide in rim layer I; or, the hibonite crystals may have condensed directly from a gas. In either case, their FeO content owes its origin to a very oxidizing gas.

We envision rim layer I as a porous aggregate of Al–Fe-oxide grains and other phases prior to massive alteration to feldspathoids, while the black rim was a massive, compact devitrified glass. This difference in consistency accounts for the sharp boundary between the two. The fact that rim layer I occasionally pinches out is explainable in this model by the fact that when a thin layer of grains accretes around a nucleus, there is no necessary reason for this coating to be continuous. If deposition of rim layer II began before the layer I coating became continuous, regions would exist where rim layer II would coat the black rim directly. In such regions, the original structure might have been a porous layer of phases characteristic of rim layer II, including a large proportion of Al–Fe-oxide, in sharp contact with the black, compact rim. The reason why the contact between the black rim and rim layer II is gradational while that between the black rim and rim layer I is sharp may be due to obscuration of the layer II/black rim contact because of a greater degree of later alteration in that region, probably related to the absence of layer I which is normally mostly feldspathoids. That the alteration intensity was greater there is suggested by the significantly greater abundance of feldspathoids where layer I is missing than either in the usual black rim or even in rim layer II.

If it is assumed that the phases in any given layer condensed from a common reservoir over a narrow range of physico-chemical conditions, the implications of the mineral assemblage in rim layer II are the same as those of layer I, that the system was far more oxidizing than a gas of solar composition. This is because andradite, containing ferric iron indicative of low solar nebular equilibration temperatures (<500 K), coexists with perovskite which disappears by reaction with a gas of solar composition above 1400 K. This interpretation is complicated, however, by the coexistence of grossular and andradite, which, as mentioned above, could indicate separate formation locations for the two garnets and may imply cold accretion of rim layer II and a lack of necessary genetic relationships between the different phases in this layer. Grossular cannot condense from a gas of solar

composition under equilibrium conditions. Thus, unless grossular formed metastably, at least one of the phases in this layer did not condense from a solar gas.

If all the phases in rim layer III condensed from the same reservoir over a narrow temperature range, oxidizing conditions are again indicated. This is suggested by the coexistence of perovskite, which disappears from a gas of solar composition above 1400 K, and a Ti–Fe-oxide containing oxidized iron, indicative of much lower temperatures in a solar gas. Oxidizing conditions are also suggested by the coexistence of apatite with perovskite. GROSSMAN and OLSEN (1974) showed that P should condense from a gas of solar composition as schreibersite, Fe_3P, above 1400 K. It is only below 1000 K where such a gas becomes oxidizing enough to stabilize phosphates relative to phosphides. Thus, co-condensation of perovskite and a phosphate could only occur in a gas phase considerably more oxidizing than a solar gas. As was the case in rim layer II, this reasoning is complicated by the coexistence in rim layer III of grossular and andradite because this implies that different phases in this layer may have formed in different reservoirs.

Many of the same mineralogical features that are present in layers I–III and which indicated that their constituents did not condense from a gas of solar composition are also present in layer IV: the presence of an Al–Fe-oxide, the presence of grossular and the coexistence of Ti–Fe-oxide with perovskite. The fact that grossular and andradite are intergrown in this layer, however, tends to weaken the argument based on coexistence of phases. The hibonite in this layer is richer in refractory Sc, Ti and Zr than that in the core, opposite to what one would expect if HAL accreted from materials in the same sequence in which they condensed from a common reservoir. Compared to hibonite in the core, this material is also richer in more volatile Fe and Mg, although this could be due to a greater degree of secondary alteration in the case of the rim hibonite.

The presence in rim layer V of grossular and an Al–Fe-oxide and the coexistence of perovskite with a Ti–Fe-oxide in this layer again suggest that some of its constituents condensed from a gas of non-solar composition. The high FeO content of the rectangular olivine crystals suggests they formed in an oxidizing environment. Again, the presence of two garnets suggests that some phases in this layer may have formed under substantially different physico-chemical conditions from others in the same layer. The unusual feature of rim layer V is the progressive increase in the abundances of pentlandite, nickel–iron and barrel-shaped olivine toward its outer edge. It would appear that, after the beginning of the gentle assembly of rim layer V, minerals typical of the matrix of Allende began to accrete at the same time as the other layer V phases. This suggests that HAL encountered a region of the dust cloud at that time in which grains of both suites of phases were mixed together. It is thus possible that grains of rim layer V phases other than pentlandite, nickel–iron and barrel-shaped olivine were incorporated in the matrix of Allende during accretion of its parent body. Assuming that such phases have the same isotopic compositions as their counterparts in other layers of HAL, the matrix of Allende could turn out to be a source of isotopically-unusual mineral grains.

CONCLUSIONS

Although it is difficult to tell whether or not the hibonite in HAL's core crystallized from a melt, the hibonite definitely reacted partially with a melt which ultimately quenched to form the black rim. This implies that, if the hibonite originally crystallized from a melt related to this one, the latter must have undergone a substantial change in composition prior to quenching. It is difficult to reconcile a liquid origin for the black rim with the LEE *et al.* (1979) model, but such an origin poses no fundamental problems in the ALLEN *et al.* (1979) model. Sectors of HAL's friable rim exist in which layer I is missing and in which the mineralogy of adjacent layers is no different from the same layers in other sectors. Layer V contains alternating olivine-rich bands and garnet-, pyroxene-rich bands and has incorporated minerals typical of the Allende matrix. For these reasons, we conclude that each of the layers of the friable rim formed by the accretion of an assemblage of condensate grains around HAL's nucleus rather than by wholesale reaction of a precursor to HAL with a nebular gas. After formation of the friable rim, HAL underwent reaction with a vapor phase which caused deposition of feldspathoids throughout the inclusion.

In the light of isotopic results on HAL (LEE *et al.*, 1979), the implication of the current work is that all of the materials which assembled to form HAL condensed from a reservoir which was low in ^{26}Al and possessed a Ca isotopic composition which had been affected by a mass fractionation process and addition of material from exotic sources. This paper thus reinforces the conclusion that the solar nebula contained isotopically-distinct reservoirs prior to and during condensation, as suggested previously (CLAYTON, 1978; LEE *et al.*, 1978). In addition, a number of mineralogical features of HAL suggest that the particular isotopic reservoir from which HAL formed did not have a solar bulk chemical composition but, instead, may have been much more oxidizing. This is suggested by the FeO content of the hibonite, the presence of the Al–Fe-oxide and, if phases within individual rim layers are cogenetic, the coexistence of perovskite with either andradite, Ti–Fe-oxide or apatite.

In the present model, all of the phases in HAL's core and rim could not have formed under the same set of physico-chemical conditions. The fact that hibonite in rim layer IV is richer in refractory Zr and Sc than that in the core suggests that the sequence of accretion of phases is not simply related to the

sequence of phases condensing from an isobaric, isochemical, monotonically-cooling gas. Rather, changes in gas phase composition, increases in temperature, large pressure changes or complex processes of separation of condensed phases from one another and later re-mixing seem to be required. It is difficult to envisage how a small, local gaseous reservoir could undergo such changes or provide an environment for such processes while still preserving its isotopic identity.

Two other Allende inclusions, C1 and EK1-4-1, are known to exhibit severe mass fractionation effects, coupled with nuclear effects due to incomplete mixing of materials from distinct nucleosynthetic sources, in the isotopic compositions of some of their major elements of low atomic number (CLAYTON and MAYEDA, 1977; WASSERBURG *et al.*, 1977). Like HAL, C1 anorthite contains much less excess ^{26}Mg than normal Allende inclusions (WASSERBURG *et al.*, 1977; ESAT *et al.*, 1978), but anorthite from EK1-4-1 has not yet been measured. Both of those inclusions also show nuclear effects in their trace elements of higher atomic number, as summarized by CLAYTON (1978). Although petrographic information as detailed as that given here for HAL is not yet available for them, and is not likely to become available ever for EK1-4-1 due to the nature of the remaining sample, it would appear from existing data that those inclusions are much more similar in petrography and mineralogy to normal Type B coarse-grained Allende inclusions than is HAL. Presumably, this reflects chemical and thermal histories for those inclusions which are less exotic than those of HAL.

Acknowledgements—Helpful discussions with R. C. ALLER, R. N. CLAYTON, A. M. DAVIS, I. D. HUTCHEON, G. MACPHERSON, R. C. NEWTON and T. TANAKA are gratefully acknowledged. We thank J. BROWN for preparing polished thin sections of superior quality. Mr ERIC LIN of the University of Toronto is thanked for Figs 8 and 13. The original manuscript was improved significantly through thoughtful reviews by A. EL GORESY, J. W. LARIMER and G. J. TAYLOR. This work was supported by funds from the National Aeronautics and Space Administration through grants NGR 14-001-249 (L.G.) and NGL 05-002-188 (G.J.W.), the Alfred P. Sloan Research Foundation (L.G.), the National Science Foundation through grant PHY76-83685 (G.J.W.), the Natural Sciences and Engineering Research Council of Canada (J.M.A.), and the Enrico Fermi Institute and Robert R. McCormick Trust (T.L.).

REFERENCES

ALLEN J. M., GROSSMAN L., DAVIS A. M. and HUTCHEON I. D. (1978) Mineralogy, textures and mode of formation of a hibonite-bearing Allende inclusion. In *Proc. 9th Lunar Planet. Sci. Conf.* pp. 1209–1233. Pergamon.

ALLEN J. M., GROSSMAN L., LEE T. and WASSERBURG G. J. (1979) Mineralogical study of an isotopically-unusual Allende inclusion (abstract). In *Lunar and Planetary Science X*. pp. 24–26. The Lunar and Planetary Institute.

BLANDER M. and FUCHS L. H. (1975) Calcium-aluminum-rich inclusions in the Allende meteorite: evidence for a liquid origin. *Geochim. Cosmochim. Acta* **39**, 1605–1619.

CLAYTON R. N. (1978) Isotopic anomalies in the early solar system. *Ann. Rev. Nucl. Part. Sci.* **28**, 501–522.

CLAYTON R. N. and MAYEDA T. K. (1977) Correlated oxygen and magnesium isotope anomalies in Allende inclusions, I: Oxygen. *Geophys. Res. Lett.* **4**, 295–298.

EL GORESY A., NAGEL K. and RAMDOHR P. (1978) The Allende meteorite: Fremdlinge and their noble relatives. In *Proc. 9th Lunar Planet. Sci. Conf.* pp. 1279–1303. Pergamon.

ESAT T. M., LEE T., PAPANASTASSIOU D. A. and WASSERBURG G. J. (1978) Search for ^{26}Al effects in the Allende FUN inclusion C1. *Geophys. Res. Lett.* **5**, 807–810.

GANGULY J. (1976) The energetics of natural garnet solid solution II. Mixing of the calcium silicate end-members. *Contrib. Mineral. Petrol.* **55**, 81–90.

GROSSMAN L. (1972) Condensation in the primitive solar nebula. *Geochim. Cosmochim. Acta* **36**, 597–619.

GROSSMAN L. (1973) Refractory trace elements in Ca–Al-rich inclusions in the Allende meteorite. *Geochim. Cosmochim. Acta* **37**, 1119–1140.

GROSSMAN L. and OLSEN E. (1974) Origin of the high-temperature fraction of C2 chondrites. *Geochim. Cosmochim. Acta* **38**, 173–187.

GROSSMAN L. and STEELE I. M. (1976) Amoeboid olivine aggregates in the Allende meteorite. *Geochim. Cosmochim. Acta* **40**, 149–155.

KEIL K. and FUCHS L. H. (1971) Hibonite [$Ca_2(Al, Ti)_{24}O_{38}$] from the Leoville and Allende chondritic meteorites. *Earth Planet. Sci. Lett.* **12**, 184–190.

LARIMER J. W. and ANDERS E. (1970) Chemical fractionations in meteorites—III. Major element fractionations in chondrites. *Geochim. Cosmochim. Acta* **34**, 367–387.

LEE T., PAPANASTASSIOU D. A. and WASSERBURG G. J. (1978) Calcium isotopic anomalies in the Allende meteorite. *Astrophys. J. Lett.* **220**, L21–L25.

LEE T., RUSSELL W. A. and WASSERBURG G. J. (1979) Ca isotopic anomalies and the lack of ^{26}Al in an unusual Allende inclusion. *Astrophys. J. Lett.* **228**, L93–L98.

MARVIN U. B., WOOD J. A. and DICKEY J. S. JR (1970) Ca–Al-rich phases in the Allende meteorite. *Earth Planet. Sci. Lett.* **7**, 346–350.

MCVICKERS R. C., FORD S. D. and DUGDALE R. A. (1962) Polishing and etching techniques for dense alumina. *J. Am. Ceram. Soc.* **45**, 199.

MINAGAWA S., SAITO T. and GEJYO T. (1968) Growth patterns on the surface of alumina grown by chemical vapor deposition. *J. Am. Ceram. Soc.* **51**, 532–533.

PEDERSON A. K. (1978) Non-stoichiometric magnesian spinels in shale xenoliths from a native iron-bearing andesite at Asuk, Disko, central west Greenland. *Contrib. Mineral. Petrol.* **67**, 331–340.

TANAKA T., DAVIS A. M., GROSSMAN L., LATTIMER J. M., ALLEN J. M., LEE T. and WASSERBURG G. J. (1979) Chemical study of an isotopically-unusual Allende inclusion (abstract). In *Lunar and Planetary Science X*. pp. 1203–1205. The Lunar and Planetary Institute.

WARK D. A. and LOVERING J. F. (1977) Marker events in the early evolution of the solar system: Evidence from rims on Ca–Al-rich inclusions in carbonaceous chondrites. In *Proc. 8th Lunar Sci. Conf.* pp. 95–112. Pergamon.

WASSERBURG G. J., LEE T. and PAPANASTASSIOU D. A. (1977) Correlated O and Mg isotopic anomalies in Allende inclusions: II. Magnesium. *Geophys. Res. Lett.* **4**, 299–302.